Inorg. Chem. **2006**, *45*, 9670–9679

Pressure Effect and Crystal Structure Reinvestigations on the Spin Crossover System: $[Fe(bt)_2(NCS)_2]$ (bt = 2,2′-Bithiazoline) Polymorphs A and B

Ana Galet,[‡] Ana Belén Gaspar,[†] M. Carmen Muñoz,[‡] Georgii Levchenko,[§] and José Antonio Real*[,†]

Institut de Ciència Molecular/Departament de Química Inorgànica, Universitat de València, Edifici de Instituts de Paterna, Apartat de Correus 22085, 46071 València, Spain, Departament de Física Aplicada, Universitat Politècnica de València, Camí de Vera s/n, 46022 València, Spain, and Donetsk Physico-Technical Institute, NAS of Ukraine, R. Luxemburg 72, 83114 Donetsk, Ukraine

Received April 28, 2006

The crystal structure of $[Fe(bt)_2(NCS)_2]$ (**A**) was determined by X-ray diffraction at 293 and at 150 K in order to analyze the structural changes associated with the spin transition. The space group is $P\bar{1}$ with $Z = 2$ at both temperatures. Lattice constants are as follows: $a = 8.5240(4)$, $b = 11.0730(6)$, $c = 12.5300(8)$ at 293 K and $a = 8.1490(4)$, $b = 11.4390(5)$, $c = 12.1270(6)$ at 150 K. The iron(II) atom lies at the center of a distorted octahedron $[FeN_6]$ defined by two bt ligands arranged in a cis conformation. The two remaining coordination positions are occupied by two isothiocyanate anions. The average bond lengths of 2.159(4) Å (293 K) and 1.951(2) Å (150 K) clearly indicate the change in spin configuration. The trigonal distortion parameter ϕ has a value of 9.6° and 5.5° at 293 and 150 K, respectively. For **A**, $\Delta V = \Delta V_{SCO} = 28$ Å^3 per formula unit and is accompanied by a hysteresis of 10 K. $\chi_M T$ vs T curves at atmospheric pressure for **A** show an abrupt spin transition with $T_c^{\downarrow} = 176$ K and $T_c^{\uparrow} = 187$ K. The thermodynamic parameters associated with the spin transition are $\Delta H = 8.4 \pm 0.4$ kJ mol^{-1} and $\Delta S = 46.5 \pm 3$ J K mol^{-1}. The thermal dependence of the magnetic susceptibility at different pressures, 0.1–0.91 GPa, points out an unusual behavior, which can only be understood in terms of a crystallographic phase transition or a change in the bulk modulus of the complex. Polymorph **B** crystallizes in the $C2/c$ space group with an average Fe–N bond length of 2.168(2) Å and $\phi = 14.7°$ at 293 K. **B** remains in the HS configuration even at pressures of 1.06 GPa.

Introduction

Spin crossover (SCO) has turned out to be a particularly appealing phenomenon as it offers the possibility of bistability, i.e., that complex molecules may exist in two different electronic states at the same temperature. The reversible change between low-spin (LS) and high-spin (HS) states driven by a variation in temperature and pressure or also by light irradiation, mainly observed in pseudo-octahedral iron(II) coordination complexes, is up to now one of the best examples of molecular bistability.[1−4] In the HS and LS states, spin crossover compounds have distinct magnetic and optical properties, dielectric constants, color, and structures. Their magnetic, dielectric, and optical properties may be altered drastically in a narrow range of temperature and pressure for cooperative transitions. Furthermore, hysteresis accompanies the first-order spin transition (ST) when the structural changes are transmitted cooperatively through the whole solid.

Because of their switching properties, the SCO materials are potentially useful for rewritable optical, thermal, or pressure memories at a nanometric scale.[5−7] To sum up the requirements that a SCO material must fulfill for the construction of devices for displays or recording data, we

* To whom correspondence should be addressed. E-mail: Jose.a.real@uv.es.
[†] Universitat de València.
[‡] Universitat Politécnica de València.
[§] Donetsk Physico-Technical Institute.

(1) Gütlich, P., Goodwin, H. A., Eds. Spin Crossover in Transition Metal Compounds. *Topics in Current Chemistry*; Springer: New York, 2004; Vols. 233, 234, 235.
(2) (a) Real, J. A.; Gaspar, A. B.; Muñoz, M. C. *J. Chem. Soc., Dalton Trans.* **2005**, 2062. (b) Gaspar, A. B.; Ksenofontov, V.; Seredyuk, M.; Gütlich, P. *Coord. Chem. Rev.* **2005**, *249*, 2661.
(3) Real, J. A.; Gaspar, A. B.; Niel, V.; Muñoz, M. C. *Coord. Chem. Rev.* **2003**, *236*, 121.
(4) Gütlich, P.; Hauser, A.; Spiering, H. *Angew. Chem., Int. Ed. Engl.* **1994**, *33*, 2024.

10.1021/ic060729u CCC: $33.50
Published on Web 11/03/2006

can say that abruptness, hysteresis, room-temperature operation, change in color, and chemical stability are necessary conditions. Nowadays, prototypes of thermal displays based on the 1D SCO polymeric systems $[Fe(4\text{-}Rtrz)_3](ClO_4)_2$, $[Fe(4\text{-}R^1trz)_{3-3x}(4\text{-}R^2trz)_{3x}](A)_2 \cdot nH_2O$, and $[Fe(4\text{-}Rtrz)_3](A^1_{1-x}A^2_x)_2 \cdot nH_2O$ (4-Rtrz = 4-substituted-1,2,4-triazole) have been described.[6,7]

During recent years, the search for new SCO functional materials suitable for practical applications has stimulated synthetic chemists to design and explore the chemical and physical properties of 1D, 2D, and 3D SCO polymers.[8−19] In this respect, the development of supramolecular chemistry and crystal engineering concepts has conveyed much of the impetus to the search for new SCO polymers. Such investigations have provided among others 3D SCO materials with pressure tunable thermal-hysteresis and baro-hysteresis loops at room temperature,[5] 3D materials exhibiting photoinduced spin transitions at room temperature,[20] and 1D materials gathering liquid crystal and spin crossover properties at around 60 °C.[21]

The occurrence of the SCO and its characteristics (T_c, hysteresis, chromism, etc.) are governed by subtle structural and electronic modifications tuned by the crystal packing, which determines the ligand field strength and the SCO behavior. These modifications depend essentially on the nature of the ligands, the noncoordinating anions, the solvent molecules, and the crystal packing. The complete control of these variables is a rather difficult task to accomplish. In addition, their effects are not always consistent from one system to another and in general are not predictable. This is particularly accentuated for monomeric complexes (0D SCO systems) as the communication between the SCO centers is achieved exclusively through intermolecular interactions, such as hydrogen bonding, aromatic $\pi-\pi$ interactions, sulfur−sulfur interactions, and even metallophilic interactions. Despite this, in some cases, it is possible to find correlations between the structure and the nature of the SCO.[1−4] One of the key problems in this kind of rationalization is the lack of systematic experimental studies. In polymeric compounds, partial or total substitution of these intermolecular interactions by covalent linkage of the metal centers leads to a more predictable control of the cooperative behavior.

Among the 0D SCO systems exhibiting abrupt spin transitions, the $[Fe(bt)_2(NCS)_2]$ complex (polymorph **A**) is an illustrative example. Since it was reported by Nelson et al. in 1976 several publications have appeared in the literature devoted to the chemical, physical, and structural characterization of both polymorphs of the complexes, hereafter **A** and **B**.[22−28] It deserves to be noted that one decade elapsed between the first report of the material[22] and the discovery of its polymorphism.[27] In contrast to polymorph **A** where $T_c\downarrow = 171.2$ K and $T_c\uparrow = 180.9$ K, polymorph **B** does not exhibit SCO behavior. Special attention has been focused in the study of the hysteresis effect in polymorph **A**.[23,25,28] It has been stated that the spin transition in **A** (powder) proceeds as a first-order phase transition involving independent domains[25] of around 50−55 molecules.[26] To clarify if the spin transition is accompanied by a crystallographic phase transition or not is still an open question, as temperature-dependent crystal structure determinations have not yet been reported. In contrast, Mössbauer experiments up to pressures of 0.2 GPa performed on **A**[28] have shown the occurrence of a linear decrease in $(\Delta T_C)^{1/2}$ with pressure as well as an increase in the HS fraction measured at low temperature with the increasing pressure.

We report herein the crystal structure determination of **A** at 150 K and a detailed analysis of the unit cell volume in the spin transition region. Structural reinvestigations of both polymorphs **A** and **B** at 293 K and the influence of hydrostatic pressures up to 1 GPa on the spin crossover properties are also discussed.

Experimental Section

Materials. $FeCl_2 \cdot 4H_2O$, KNCS, and absolute ethanol were purchased from commercial sources and used as received. The 2,2′-bithiazoline was synthesized as described in the literature.[27]

(5) Galet, A.; Gaspar, A. B.; Muñoz, M. C.; Bukin, G. V.; Levchenko, G.; Real, J. A. *Adv. Mater.* **2005**, *17*, 2949.
(6) (a) Kahn, O.; Martinez, C. J. *Science* **1998**, *279*, 44. (b) Kahn, O.; Kröber, J.; Jay, C. *Adv. Mater.* **1992**, *4*, 718.
(7) García, Y.; Ksenofontov, V.; Gütlich, P. *Hyperfine Interact.* **2002**, *139*, 543.
(8) Niel, V.; Martinez-Agudo, J. M.; Muñoz, M. C.; Gaspar, A. B.; Real, J. A. *Inorg. Chem.* **2001**, *40*, 3838.
(9) Niel, V.; Galet, A.; Gaspar, A. B.; Muñoz, M. C.; Real, J. A. *Chem. Commun.* **2003**, 1248.
(10) Galet, A.; Muñoz, M. C.; Martínez, V.; Real, J. A. *Chem. Commun.* **2004**, 2268.
(11) Garcia, Y.; Kahn, O.; Rabardel, L.; Chansou, B.; Salmon, L.; Tuchagues, J. P. *Inorg. Chem.* **1999**, *38*, 4663.
(12) (a) van Koningsbruggen, P. J.; Garcia, Y.; Kooijman, H.; Spek, A. L.; Haasnoot, J. G.; Kahn, O.; Linares, J.; Codjovi, E.; Varret, F. *J. Chem. Soc., Dalton Trans.* **2001**, 466. (b) Grunert, C. M.; Schweifer, J.; Weinberger, P.; Linert, W.; Mereiter, K.; Hilscher, G.; Müller, M.; Wiesinger, G.; van Koningsbruggen, P. J. *Inorg. Chem.* **2004**, *43*, 155.
(13) Galet, A.; Niel, V.; Muñoz, M. C.; Real, J. A. *J. Am. Chem. Soc.* **2003**, *125*, 14224.
(14) Niel, V.; Thompson, A. L.; Galet, A.; Muñoz, M. C.; Goeta, A. E.; Real, J. A. *Angew. Chem., Int. Ed.* **2003**, *42*, 3760.
(15) Niel, V.; Muñoz, M. C.; Gaspar, A. B.; Levchenko, G., Real, J. A. *Chem.—Eur. J.* **2002**, *8*, 2446.
(16) Real, J. A.; Andrés, E.; Muñoz, M. C.; Julve, M., Granier, T.; Bousseksou, A.; Varret, F. *Science* **1995**, *268*, 265.
(17) Halder, G. J.; Kepert, C. J.; Moubaraki, B.; Murray, K. S.; Cashion, J. D. *Science* **2002**, *298*, 1762.
(18) van Koningsbruggen, P. J.; Garcia, Y.; Kahn, O.; Fournès, L.; Kooijman, H.; Haasnoot, J. G.; Moscovici, J.; Provost, K.; Michalowicz, A.; Renz, F.; Gütlich, P. *Inorg. Chem.* **2000**, *39*, 1891.
(19) Schweifer, J.; Weinberger, P.; Mereiter, K.; Boca, M.; Reichl, C.; Wiesinger, G.; Hilscher, G.; van Koningsbruggen, P. J.; Kooijman, H.; Grunert, M.; Linert, W. *Inorg. Chim. Acta* **2002**, *339*, 297.
(20) Bonhommeau, S.; Molnár, G.; Galet, A.; Zwick, A.; Real, J. A.; McGarvey, J. J.; Bousseksou, A. *Angew. Chem., Int. Ed. Engl.* **2005**, *44*, 4069.
(21) Seredyuk, M.; Gaspar, A. B.; Ksenofontov, V.; Reiman, S.; Galyametdinov, Y.; Haase, W.; Renstchler, E.; Gütlich, P. *Chem. Mater.* **2006**, *18*, 2513.
(22) Nelson, J.; Nelson, S. M.; Perry, W. D. *J. Chem. Soc., Dalton Trans.* **1976**, 1282.
(23) Bradley, G.; McKee, V.; Nelson, S. M.; Nelson, J. *J. Chem. Soc., Dalton Trans.* **1978**, 522.
(24) König, E.; Ritter, G.; Irler, W. *Inorg. Chim. Acta* **1979**, *37*, 169.
(25) Müller, E. W.; Spiering, H.; Gütlich, P. *J. Chem. Phys.* **1983**, *79*, 1439.
(26) Kulshreshtha, S. K.; Sasikala, R.; König, E. *Chem. Phys. Lett.* **1986**, *123*, 215.
(27) Ozarowski, A.; McGarvey, B. R.; Sarkar, A. B.; Drake, J. E. *Inorg. Chem.* **1988**, *27*, 628.
(28) König, E.; Ritter, G.; Grünsteudel, H.; Dengler, J.; Nelson, J. *Inorg. Chem.* **1994**, *33*, 837.

Synthesis of $[Fe(bt)_2(NCS)_2]$ (A and B). The synthetic method used in the synthesis of $[Fe(bt)_2(NCS)_2]$ (**A**) and $[Fe(bt)_2(NCS)_2]$ (**B**) varies slightly from that described by Ozarowski et al.[27] The synthesis was carried out under an argon atmosphere. To a solution of $FeCl_2 \cdot 4H_2O$ (0.2 g, 1 mmol) in absolute ethanol (15 mL) was added an ethanolic solution (15 mL) of KNCS (0.2 g, 2 mmol). The solution was stirred for 15 min, and the resulting precipitate (KCl) was filtered off. The colorless solution containing Fe/NCS^- (1:2) was heated to 40 °C and added dropwise to a hot solution (40 °C) of 2,2′-bithiazoline (0.26 g, 1.5 mmol) in absolute ethanol (25 mL) changing the color of the solution to violet. The quickly formed precipitate **A** was filtered off, and the solution was heated until reduced to one-third of the total volume. Next, it was allowed to evaporate under argon for 1 week, giving crystals of **A** (elongated black parallelepipeds) and **B** (black octahedral with cutoff corners) suitable for X-ray studies. Results for **A** follow. Yield: 50%. Anal. Calcd for $C_{14}H_{16}N_6S_6Fe$: C, 32.56; H, 3.10; N, 16.28. Found: C, 32.71; H, 3.14; N, 16.47. Results for **B** follow. Yield: 30%. Anal. Calcd for $C_{14}H_{16}N_6S_6Fe$: C, 32.56; H, 3.10; N, 16.28. Found: C, 32.43; H, 3.09; N, 16.11.

X-ray Crystallographic Study. Diffraction data for all complexes were collected with a Nonius Kappa-CCD (charge-coupled device) single-crystal diffractometer using Mo Kα radiation (λ = 0.710 73 Å). A multiscan absorption correction was found to have no significant effect on the refinement results. The structures were solved by direct methods using SHELXS-97 and refined by full-matrix least-squares on F^2 using SHELXL-97.[29] All non-hydrogen atoms were refined anisotropically.

Differential Scanning Calorimetry (DSC). Calorimetric measurements have been performed on **A** using a differential scanning calorimeter (Mettler Toledo DSC 821e). Low temperatures were obtained with an aluminum block that was attached to the sample holder, refrigerated with a flow of liquid nitrogen, and stabilized at a temperature of 110 K. The sample holder was kept in a drybox under a flow of dry nitrogen gas to avoid water condensation. The measurements were carried out using around 20 mg of a powdered sample sealed in aluminum pans with a mechanical crimp. Temperature and heat flow calibrations were made with standard samples of indium by using its melting (429.6 K, 28.45 J g^{-1}) transition. An overall accuracy of 0.2 K in the temperature and 2% in the heat capacity is estimated.

Magnetic Susceptibility Measurements under Hydrostatic Pressure. Variable-temperature magnetic susceptibility measurements were performed on small single crystals by using a Quantum Design MPMS2 SQUID susceptometer equipped with a 5.5 T magnet and operating at 1 T and 1.8−375 K. The hydrostatic pressure cell made of hardened beryllium bronze with silicon oil as the pressure transmitting medium operates in the pressure range 10^5 Pa < P < 1.2 GPa (accuracy ± 0.025 GPa). Cylindrically-shaped powder sample holders with dimensions of 1 mm in diameter and 5−7 mm in length were used. The pressure was measured using the pressure dependence of the superconducting transition temperature of a built-in pressure sensor made of high purity tin.[30] Experimental data were corrected for diamagnetism using Pascal's constants.

Results

Crystal Structure of A and B. Crystal structure determinations were performed at 293 K for **A** and **B**, and at 150 K for **A**. Complexes **A** and **B** crystallize in the triclinic and monoclinic space groups, $P\bar{1}$ and $C2/c$, respectively. A selection of crystallographic data, bond distances, and angles is given in Tables 1 and 2. Figures 1 and 2 display the molecular structure of polymorph **A** and **B**, respectively, together with the corresponding atom numbering scheme. The structure of both is made up of discrete neutral $[Fe(bt)_2(NCS)_2]$ units. The iron(II) atom lies at the center of a distorted octahedron $[FeN_6]$ defined by two bt ligands arranged in a cis conformation. The two remaining coordination positions are occupied by two isothiocyanate anions. At 293 K, the trigonal distortion parameter ϕ has a value of 9.6° and 14.7° for **A** and **B**, respectively, which denotes a stronger distortion from the octahedron toward a trigonal polyhedron in **B**. (The average trigonal distortion parameter, ϕ, can be defined as $\phi = \sum(|60 - \theta|)/24$, where θ represents the trigonal angles defined by two opposed faces of the octahedron, giving a total of 24 trigonal angles.)[49]

Table 1. Crystal Data for Polymorphs **A** and **B**

	A (293 K)	**A** (150 K)	**B** (293 K)
formula	$C_{14}H_{16}N_6S_6Fe$		
fw	516.54		
crystal system	triclinic	triclinic	monoclinic
space group	$P\bar{1}$	$P\bar{1}$	$C2/c$
a (Å)	8.5240(4)	8.1490(4)	18.7470(8)
b (Å)	11.0730(6)	11.4390(5)	10.7970(5)
c (Å)	12.5300(8)	12.1270(6)	11.6000(5)
α (deg)	96.816(3)	93.516(2)	
β (deg)	91.811(3)	95.411(2)	117.439(2)
γ (deg)	106.256(2)	107.400(2)	
V (Å^3)	1124.74(11)	1069.12(9)	837.5(4)
Z	2	2	4
D_c (mg cm^{-3})	1.525	1.605	1.646
F(000)	528	528	1056
μ (Mo K$_\alpha$) (mm^{-1})	1.239	1.304	1.338
crystal size (mm)	0.05 × 0.06 × 0.09	0.05 × 0.06 × 0.09	0.04 × 0.05 × 0.06
temperature (K)	293(2)	150(2)	293(2)
no. of total reflections	5092	4769	2355
no. of reflections [$I > 2\sigma(I)$]	2880	3968	2050
R_1[a] [$I > 2\sigma(I)$]	0.0569	0.0392	0.0285
$wR^{a,b}$	0.1254	0.1040	0.713
S	1.060	0.997	0.997

[a] $R_1 = \sum||F_o| - |F_c||/\sum |F_o|$; $wR = [\sum[w(F_o^2 - F_c^2)^2]/\sum [w(F_o^2)^2]]^{1/2}$. [b] $w = 1/[\sigma^2(F_o^2) + (mP)^2 + nP]$ where $P = (F_o^2 + 2F_c^2)/3$; $m = 0.0723$ (**1** (293 K)), 0.0666 (**1** (150 K)), and 0.0582 (**2**); and $n = 0.0670$ (**1** (293 K)), 0.3023 (**1** (150 K)), and 9.5354 (**2**).

(29) Sheldrick, G. M. SHELX97: Program for Crystal Structure Determination. University of Gottingen, Germany, 1997.
(30) Baran, M.; Dyakonov, V. P.; Gladczuk, L.; Levchenko, G. G.; Piechota, S.; Szymczak, G. *Physica C* **1995**, *241*, 383.
(31) Wiehl, L.; Kiel, G.; Köhler, C. P.; Spiering, H.; Gütlich, P. *Inorg. Chem.* **1986**, *25*, 1565.
(32) Real, J. A.; Gallois, B.; Granier, T.; Suez-Panamá, F.; Zarembowitch, J. *Inorg. Chem.* **1992**, *31*, 4972. (b) Ksenofontov, V.; Gaspar, A. B.; Levechenko, G.; Fitzsimmons, B.; Gütlich, P. *J. Phys. Chem. B* **2004**, *108*, 7723.
(33) Gütlich, P.; Ksenofontov, V.; Gaspar, A. B. *Coord. Chem. Rev.* **2005**, *249*, 1811.
(34) Ksenofontov, V.; Gaspar, A. B.; Gütlich, P. *Top. Curr. Chem.* **2004**, *235*, 23.
(35) Usha, S.; Srinivasan, R.; Rao, C. N. R. *Chem. Phys.* **1985**, *100*, 447.
(36) Köhler, C. P.; Jakobi, R.; Meissner, E.; Wiehl, L.; Spiering, H.; Gütlich, P. *J. Phys. Chem. Solids* **1990**, *51*, 239.
(37) Romstedt, H.; Hauser, A.; Spiering, H. *J. Phys. Chem. Solids* **1998**, *59*, 265.
(38) Adler, P.; Wiehl, L.; Meissner, E.; Köhler, C. P.; Spiering, H.; Gütlich, P. *J. Phys. Chem. Solids* **1987**, *48*, 517.
(39) (a) König, E.; Madeja, K. *Inorg. Chem.* **1967**, *6*, 48. (b) König, E.; Madeja, K.; Watson, J. K. *J. Am. Chem. Soc.* **1968**, *90*, 1146.
(40) Gallois, B.; Real, J. A.; Hauw, C.; Zarembovitch, J. *Inorg. Chem.* **1990**, *29*, 1152.

Table 2. Selected Bond Lengths (Å), Intermolecular Contacts (Å), and Angles (deg) for **A** and **B**

	A (293 K)	**A** (150 K)	**B**
Fe−N(1)	2.211(3)	1.954(2)	2.2235(2)
Fe−N(2)	2.200(3)	1.961(2)	2.199(2)
Fe−N(3)	2.239(3)	1.954(2)	
Fe−N(4)	2.177(3)	1.961(2)	
Fe−N(5)	2.068(4)	1.938(2)	2.082(2)
Fe−N(6)	2.059(4)	1.940(2)	
average Fe−N distance	2.159(4)	1.951(2)	2.168(2)
N(1)−Fe−N(2)	74.11(12)	80.48(8)	74.72(6)
N(1)−Fe−N(3)	89.97(12)	96.15(8)	
N(1)−Fe−N(4)	95.23(13)	95.10(8)	
N(1)−Fe−N(5)	162.60(13)	171.07(8)	162.44(7)
N(1)−Fe−N(6)	89.04(14)	86.51(8)	
N(2)−Fe−N(3)	88.55(12)	93.19(8)	
N(2)−Fe−N(4)	159.34(14)	171.42(8)	
N(2)−Fe−N(5)	88.55(13)	91.19(8)	87.72(7)
N(2)−Fe−N(6)	106.11(13)	94.93(8)	
N(3)−Fe−N(4)	73.54(12)	79.90(8)	
N(3)−Fe−N(5)	88.07(13)	87.47(8)	
N(3)−Fe−N(6)	164.41(13)	171.77(8)	
N(4)−Fe−N(5)	100.78(13)	93.57(8)	
N(4)−Fe−N(6)	91.06(14)	92.12(8)	
N(5)−Fe−N(6)	97.4(2)	91.03(8)	

S···S contacts	**A** (293 K)	**A** (150 K)	**B**
S(5)[a]···S(1)	3.340(2)	3.2719(8)	
S(6)[b]···S(2)	3.941(2)	3.597(9)	
S(6)[c]···S(6)	3.908(3)	4.1783(11)	
S(5)[d]···S(3)	4.576(2)	3.8415(11)	
S(5)[e]···S(4)	4.028(2)	3.6434(10)	
S(2)[f]···S(1)			3.7954(7)
S(3)[g]···S(2)			3.8080(7)
S(3)[h]···S(1)			3.3863(7)
S(2)[i]···S(2)			3.4883(9)

[a] $1+x, 1+y, z$. [b] $1-x, 1-y, 2-z$. [c] $-x, 1-y, 1-z$. [d] $1+x, y, z$. [e] $1-x, -y, 1-z$. [f] $1-x, -y, 1-z$. [g] $1-x, 1-y, 1-z$. [h] $x+1/2, 1/2-y, z+1/2$. [i] $1-x, y, 3/2-z$.

For **A**, at 293 K, the Fe−N bond lengths involving NCS$^-$ groups [Fe−N(5) = 2.068(4) Å and Fe−N(6) = 2.059(4) Å] are much shorter than those involving the bt ligands [Fe−N(1) = 2.211(3) Å, Fe−N(2) = 2.200(3) Å, Fe−N(3) = 2.239(3) Å, Fe−N(4) = 2.177(3) Å]. These bond distances are typical for iron(II) complexes in the high-spin state, in agreement with the magnetic measurements at room temperature. The isothiocyanate ligands are almost linear [N(5)−C(13)−S(5) = 178.9(2)° and N(6)−C(14)−S(6) = 178.1(2)°] and slightly tilted with respect to the corresponding Fe−N(5) and Fe−N(6) bonds by 16.2° and 1.2°, respectively.

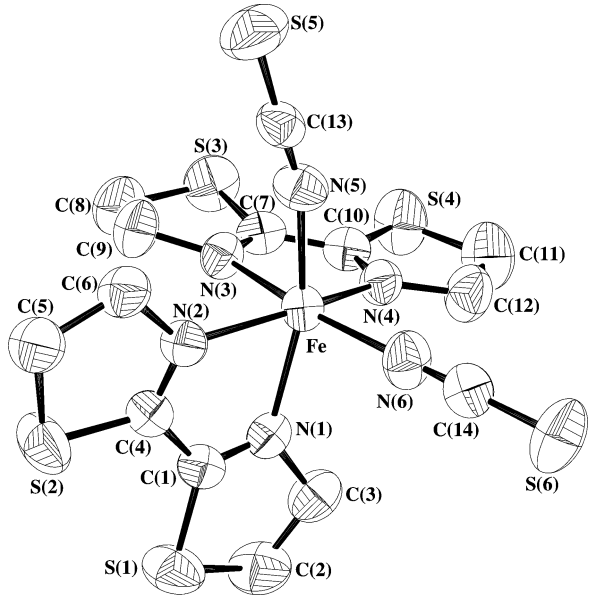

Figure 1. OTERP diagram of [Fe(bt)$_2$(NCS)$_2$] polymorph **A** at 293 K with the corresponding atom numbering scheme. Displacement ellipsoids are shown at 50% probability levels.

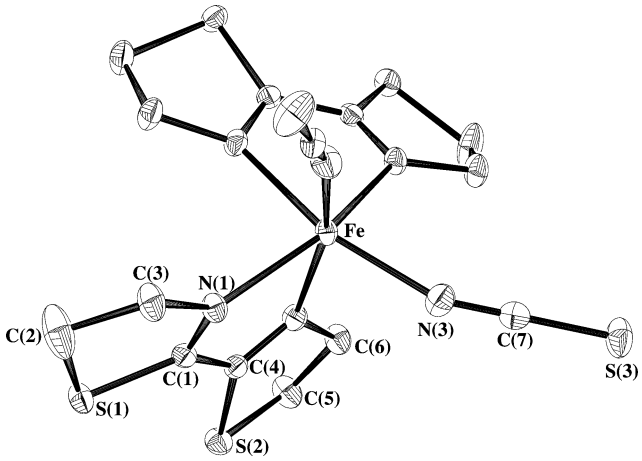

Figure 2. OTERP diagram of [Fe(bt)$_2$(NCS)$_2$] polymorph **B** at 293 K with the corresponding atom numbering scheme. Displacement ellipsoids are shown at 50% probability levels.

This crystal data at 293 K for **A** agrees very well with the earlier findings reported in ref 28.

The crystal packing of **A** can be described as formed by chains of monomers running parallel to the [110] direction. Figure 3 displays a view of the crystal packing along the [100] direction. Within a chain, there are very short S···S intermolecular contacts established between the atom S(1) of the bithiazoline ring and the atom S(5)^i of the isothiocyanato group of a consecutive complex molecule. The distance S(1)···S(5)^i = 3.340(2) Å is remarkably shorter than the sum of the van der Waals radii of two S atoms (3.7 Å), indicating the occurrence of strong S···S interactions. There are also four much weaker S···S contacts between the chains, ranging 3.908(3)−4.576(2) Å (Table 2).

No change in the space group occurs at 150 K in this polymorph. At 150 K, an average bond length of 1.951(2) Å clearly denotes the change in the spin configuration. The more symmetric octahedral coordination sphere inherent

(41) Matouzenko, G. S.; Bousseksou, A.; Lecoq, S.; van Koningsbruggen, P. J.; Perrin, M.; Kahn, O.; Collet, A. *Inorg. Chem.* **1997**, *36*, 5869.
(42) (a) Moliner, N.; Gaspar, A. B.; Muñoz, M. C.; Niel, V.; Cano, J.; Real, J. A. *Inorg. Chem.* **2001**, *40*, 3986. (b) Gaspar, A. B.; Muñoz, M. C.; Moliner, N.; Ksenofontov, V.; Levchenko, G.; Gütlich, P.; Real, J. A. *Monatsh. Chem.* **2003**, *134*, 285.
(43) Thompson, A. L.; Goeta, A. E.; Real, J. A.; Galet, A.; Muñoz, M. C. *Chem. Commun.* **2004**, 1390.
(44) Hauser, A.; Gütlich, P.; Spiering, H. *Inorg. Chem.* **1986**, *25*, 4245.
(45) Ksenofontov, V.; Spiering, H.; Schreiner, A.; Levchenko, G.; Goodwin, H. A.; Gütlich, P. *J. Phys. Chem. Solids* **1999**, *60*, 393.
(46) Ksenofontov, V.; Levchenko, G. G.; Spiering, H.; Gütlich, P.; Lètard, J. F.; Bouhedja, Y.; Kahn, O. *Chem. Phys. Lett.* **1998**, *294*, 545.
(47) Guionneau, P.; Brigouleix, C.; Barrans, Y.; Goeta, A. E.; Létard, J.-F.; Howard, J. A. K.; Gaultier, J.; Chasseau, D. *C. R. Acad. Sci. Paris Chemie/Chemistry* **2001**, *4*, 161.
(48) Guionneau, P.; Marchivie, M.; Garcia, Y.; Howard, J. A. K.; Chasseau, D. *Phys. Rev. B* **2005**, *72*, 214408.
(49) Purcell, K. F. *J. Am. Chem. Soc.* **1979**, *101*, 5147.

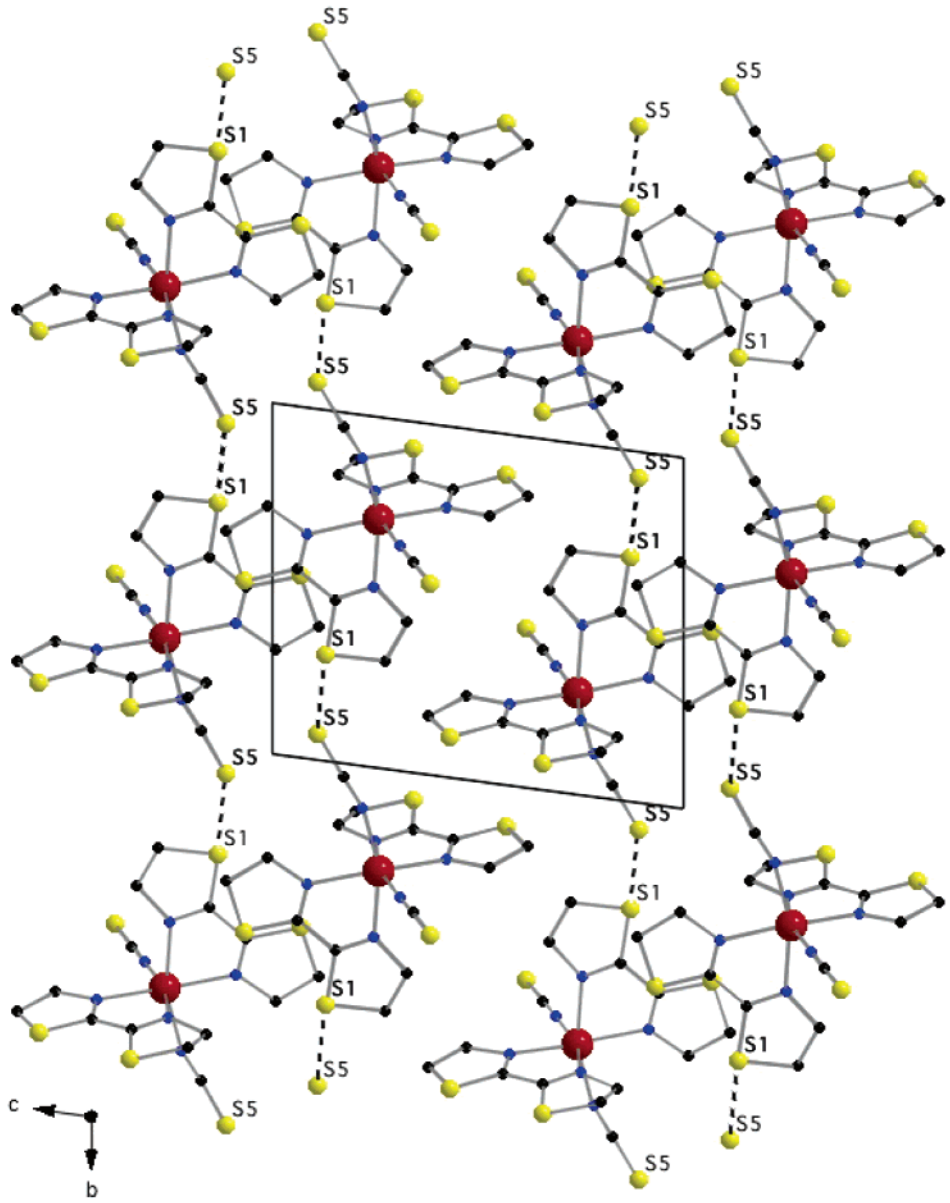

Figure 3. View of the crystal packing of **A** in the (*b*, *c*) plane. The intermolecular S···S contacts between mononuclear units in all directions are denoted as dotted lines.

to the LS configuration is also reflected in the angles N(1)−Fe−N(5), N(2)−Fe−N(4), and N(3)−Fe−N(6), their average being 171.42(8)° (162.12(14)° at 293 K). Indeed, the trigonal distortion parameter ϕ is equal to 5.5° in the LS state. The S···S contacts become notably shorter at this temperature: S(1)···S(5)^{i} = 3.2719(8) Å, S(2)···S(6)^{ii} = 3.597(9) Å, S(3)···S(5)^{iv} = 3.8415(11) Å, S(4)···S(5)^{v} = 3.6434(10) Å, and S(6)···S(6)^{iii} = 4.1783(11) Å. As a consequence, the cell parameters *a* and *c* contract by 0.3713(9) and 0.4030(2) Å, respectively, and *b* expands by 0.3659(9) Å (Table 2).

Figure 4a illustrates the variation in the unit cell volume as a function of the temperature, in the cooling and warming modes, which has been derived from multitemperature X-ray single crystal determinations successfully performed on this polymorph. At 200 K, a volume of 1123 Å^3 indicates a HS configuration for the Fe(II) ions. Practically no change in the volume is observed until the vicinity of $T_c\downarrow$ (≈170 K), where within 5 K the volume is reduced by 56 Å^3 and remains constant down to 150 K (1068 Å^3). The volume cell variation shows ca. 10 K of hysteresis width, like that observed in the magnetic susceptibility as well as in the heat capacity (vide infra). At 180 K, the volume again reaches 1123 Å^3 (HS configuration). The change in volume ΔV of the unit cell can be separated into two contributions: the volume change, ΔV_{SCO}, resulting from the spin crossover and the lattice thermal contraction ΔV_T.[31] Figure 4b represents the thermal variation of the lattice parameters. As can be seen, the thermal contraction (expansion) (ΔV_T) is negligible between 293 and 190 K, as *a*, *b*, and *c* remain constant; only in the vicinity of T_c does an appreciable modification of the cell parameters take place. Therefore, the ΔV = 56 Å^3 can be considered to be equal to ΔV_{SCO}, which corresponds to 28 Å^3 per formula unit. Typical ΔV_{SCO} values are in the range 15−30 Å^3 for most mononuclear and polynuclear compounds.[13,31,32]

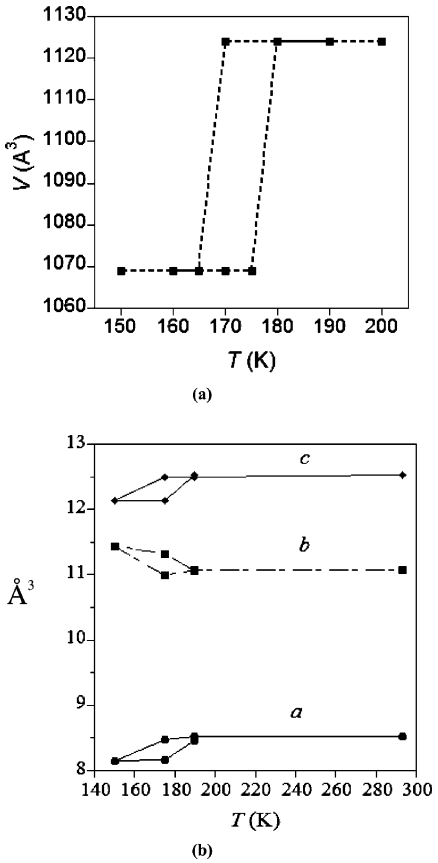

Figure 4. (a) Volume change in the unit cell as a function of the temperature for **A**. (b) Temperature dependence of the lattice parameters *a*, *b*, and *c* for **A**.

As far as the molecular structure of polymorph **B** is concerned, it is very similar to that of polymorph **A**. The average bond length, 2.168(2) Å, is just 0.009(4) Å larger than that observed for **A** at 293 K. The major difference between both polymorphs is found to be the parameter of trigonal distortion, ϕ, which is 5.1° greater for **B** ($\phi = 14.7°$). The crystal packing of **B** is rather different from that of polymorph **A** (Figure 5). Each complex molecule interacts with its four nearest neighbors through six strong, short S···S contacts (four S(1)···S(3)^{viii} = 3.3863(7) Å and two S(2)···S(2)^{ix} = 3.4883(9) Å) defining corrugated layers, which lie in the *ac* plane and stack along the *b* direction. The planes are related by the ($x + 1/2$, $y + 1/2$, 0) symmetry operation.

Magnetic Properties of A and B under Applied Hydrostatic Pressure. The thermal dependence of the $\chi_M T$ product (χ_M is magnetic susceptibility, T is temperature) performed at 1 bar (10^5 Pa) for **A** is depicted in Figure 5 together with the thermal dependence of the heat capacity, C_p, obtained from DSC (differential scanning calorimetry) measurements. The critical temperature at which the spin transition arises for the cooling and warming modes, $T_c^{\downarrow} =$ 176 K and $T_c^{\uparrow} =$ 187 K, matches very well with that reported in the literature.[25−27] The thermodynamic parameters evaluated from differential scanning calorimetry measurements, $\Delta H = 8.4 \pm 0.4$ kJ mol^{-1} and $\Delta S = 46.5 \pm 3$ J K mol^{-1}, are in agreement with those reported by Kulshreshtha et al.[26]

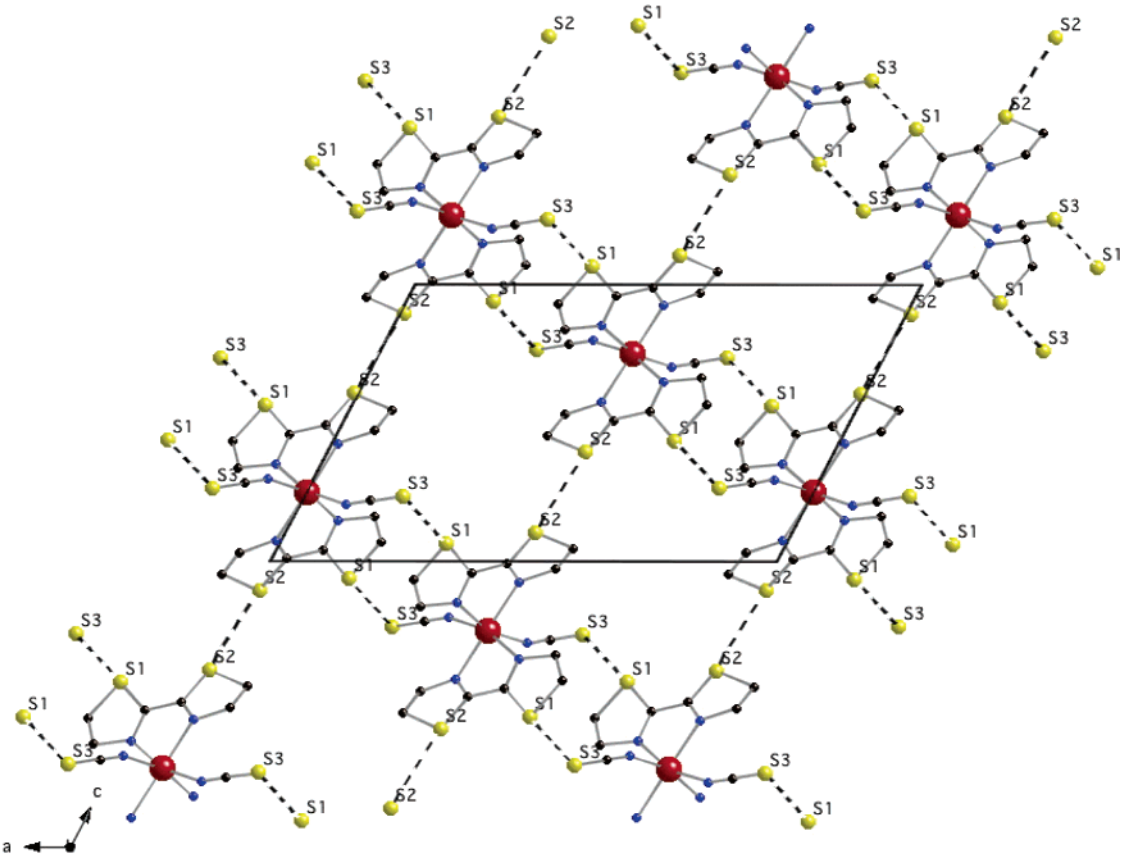

Figure 5. View of the crystal packing of **B** in the (*a*, *c*) plane. The intermolecular S···S contacts between mononuclear units in all directions are denoted as dotted lines.

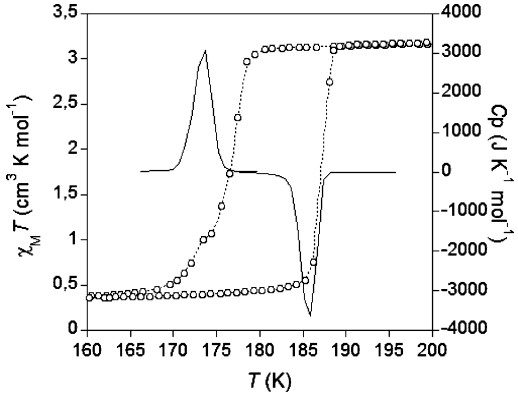

Figure 6. Temperature-dependent magnetic susceptibility (10^5 Pa) (open circles) and DSC measurements performed at a rate of 1 K/min for **A** (solid line).

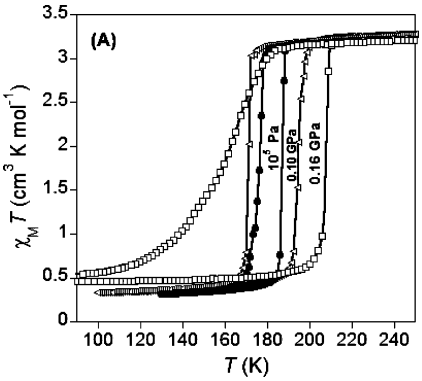

Figure 7. Temperature-dependent magnetic susceptibility measurements performed at 10^5 Pa, 0.10 GPa, and 0.16 GPa for **A** (rate of measurements: 1 K/min).

The pressure influence on the spin transition behaviors of **A** and **B** was monitored by performing magnetic susceptibility (χ_M) measurements at the rate of 1 K/min. Figures 6−10 show a representative set of such measurements expressed as the thermal dependence of the $\chi_M T$ product at different pressures.

Figures 7 and 8 display the magnetic behavior of **A** at relatively low pressures, ca. 0.1−0.34 GPa. For $P = 0.1$ GPa, the transition remains steep and the critical temperature for the cooling and warming modes changes: $T_c^{\downarrow} = 171$ K and $T_c^{\uparrow} = 195$ K, respectively. Surprisingly, the thermal hysteresis dramatically increases, $\Delta T \approx 24$ K. This change in the hysteresis loop is still much more pronounced at pressures of 0.16 GPa. Indeed, the $T_c^{\downarrow}$ is shifted downward, being centered at around 157 K, and $T_c^{\uparrow}$ is equal to 208 K ($\Delta T \approx 51$ K). Another remarkable fact is the decrease in abruptness of the spin transition in the cooling mode, in contrast to the transition in the warming mode, which remains steep. A further increase in the pressure up to 0.19 GPa results in an increase in the hysteresis loop width ($\Delta T \approx 71$ K); the spin transition in the cooling mode becomes more gradual in comparison with that observed at 0.16 GPa. It is also worth noting the increase in the residual HS fraction as the pressure increases. In this respect, the percentage of molecules in the HS state at low temperature (5 K) and at 10^5 Pa inferred from the $\chi_M T$ value is ca. 9%, and it is 16% at 0.19 GPa. Figure 8b depicts the hysteresis cycle experiments performed

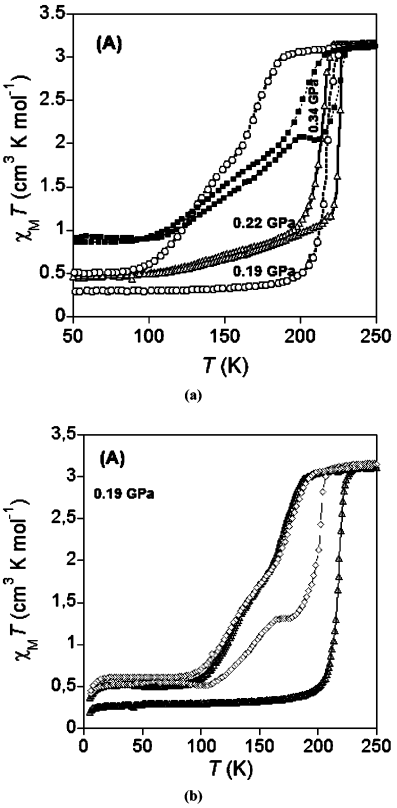

Figure 8. (a) Temperature-dependent magnetic susceptibility measurements performed at 0.19, 0.22, and 0.34 GPa for **A** (rate of measurements: 1 K/min). (b) $\chi_M T$ vs T at 0.19 GPa; the first hysteresis cycle is denoted with black triangles and the second hysteresis cycle as a gray rhombus.

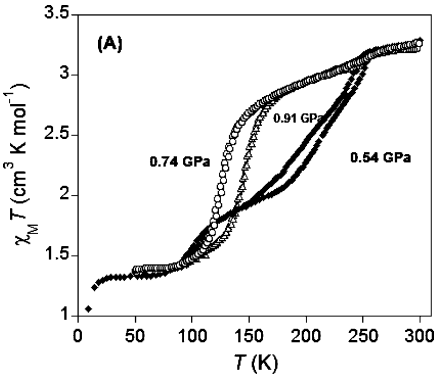

Figure 9. Temperature-dependent magnetic susceptibility measurements performed at 0.54, 0.74, and 0.91 GPa for **A** (rate of measurements: 1 K/min).

at 0.19 GPa. As can be seen, the width of the hysteresis is reduced by around 23 K in the second cycle. Such a decrease in the hysteresis width with the increasing number of cycles has been observed also at 0.16 and 0.22 GPa.

When the pressure reaches 0.22 GPa, surprisingly, the spin transition resembles that observed at 10^5 Pa; however, it is shifted upward and loses its original well-defined square shape. The hysteresis width $\Delta T \approx 14$ K ($T_c^{\downarrow} = 210$ K and $T_c^{\uparrow} = 224$ K) is similar to that observed at atmospheric pressure ($\Delta T \approx 11$ K). Increasing the pressure to 0.34 GPa provokes a drastic change in the spin crossover behavior. At 210 K, the spin transition appears quite steep with a 20 K hysteresis loop; however, below ca. 190 K, it transforms into a gradual one with ca. 30% of molecules remaining in

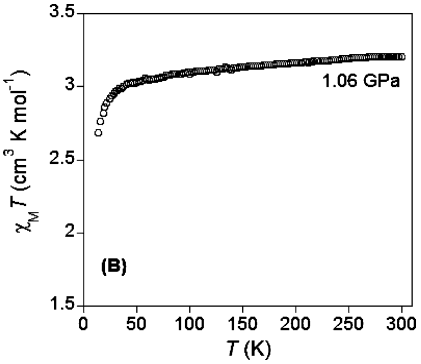

Figure 10. Temperature-dependent magnetic susceptibility measurements performed at 1.06 GPa for **B** (rate of measurements: 1 K/min).

the HS state at low temperature. A further increase in the pressure to 0.54, 0.74, and 0.91 GPa discloses the appearance of a new stable phase in which only 50% of the Fe(II) ions undergo a spin transition (Figure 9). Seemingly, the transformation to the new phase is completely accomplished at 0.74 GPa ($T_{1/2} \approx 120$ K). In fact, at 0.91 GPa, the percentage of molecules showing a change in the spin state remains constant and $T_{1/2}$ is shifted to 145 K. Reversibility of these measurements was checked after completely relaxing the pressure because the magnetic behavior of **A** at 10^5 Pa was perfectly reproducible. Moreover, the magnetic behavior of **A** in the range 10^5 Pa to 0.74 GPa was investigated in two independent experiments obtaining exactly the same results.

The pressure dependence of $T_c(P)$ can be expressed as follows:

$$T_c(P) = T_c + P(\Delta V_{HL}/\Delta S_{HL}) \quad (1)$$

or

$$dT_c/dP = \Delta V_{HL}/\Delta S_{HL} \quad (2)$$

In general, SCO systems follow this linear dependence of $T_c(P)$ versus P.[33,34] Furthermore, the mean field theory of phase transitions in SCO compounds predicts a decrease in the hysteresis width and in the slope of the transition curve with increasing pressure.[33−38] The hysteresis vanishes at a critical pressure, and at even higher pressures, the transition transforms into a second-order gradual phase transition. However, there are several SCO systems in which the effect of pressure on the SCO behavior cannot be adequately described by this theory.[33,34] Occurrence of structural phase transitions and a change in the bulk modulus of the materials under applied pressure has been proposed for the anomalous behavior observed, e.g., an increase in the hysteresis width and nonlinear hysteretic behavior of $T_c(P)$ versus P.[5,33,34,45] The response of polymorph **A** under applied pressures is quite unexpected and only can be understood in terms of a crystallographic phase transition or a change in the bulk modulus of the material. An understanding of such unexpected pressure effects will be possible from crystal structure determination under applied pressure and, of course, at variable temperature.

At 293 K, the bond length average for compound **B** is 2.1684(17) Å, which indicates that the compound is in the HS configuration and agrees with a $\chi_M T$ of 3.20 cm^3 K mol^{-1} (Figure 10). The magnetic properties of the complex at atmospheric pressure are identical to those observed at 1.06 GPa. Consequently, no spin transition is observed under such a relatively high pressure. The decrease in $\chi_M T$ below 50 K is due to the zero field splitting of the iron(II) ions in the $S = 2$ state.

Discussion

The effect of polymorphism on the SCO behavior has been known since the first studies on the classical system [Fe(L)$_2$(NCX)$_2$], where L is phen (X = S, Se) or 2,2′-bipy (X = S), by König and co-workers.[39] In these instances, the difference between polymorphs arises from the different preparative methods used (extracted, precipitated, etc.), which influence the abruptness and the residual HS molecules at temperatures below T_c. For instance, the so-called polymorph I of the phen derivative, obtained from [Fe(phen)$_3$](NCX)$_2$ via Soxhlet extraction with acetone for ca. 3 weeks, displays a complete and quite abrupt SCO at $T_c \approx 176$ K with a hysteresis of 1 K. In contrast, the precipitated form (polymorph II) is less cooperative. It displays a very narrow hysteresis, and around 16% of molecules remain HS below $T_c \approx 177$ K. Magnetic and crystallographic studies on single crystals, obtained 20 years later from slow diffusion methods, confirmed that the precipitated form and the single crystals correspond to the same polymorph II (space group *Pbcn*).[40] However, as far as we know, the first structurally characterized example of polymorphism in an iron(II) SCO compound corresponds to the system [Fe(bt)$_2$(NCS)$_2$].[27] Soon after, other important examples of structurally characterized polymorphisms appeared in the literature, such as the three polymorphs of the *fac*-[Fe(dppa)(NCS)$_2$] complex (dppa = 3-aminopropyl)bis(2-pyridylmethyl)amine)[41] and the two polymorphs of the system [Fe(abpt)$_2$(NCX)$_2$] (abpt = 4-amino-3,5-bis(pyridin-2-yl)-1,2,4-triazole and X = S or Se).[42] In the former system, polymorph **A** ($P\bar{1}$) presents a SCO with $T_c \approx 150$ K, polymorph **B** ($P2_1/c$) is paramagnetic, and polymorph **C** (*Pbca*) undergoes an abrupt SCO centered at 116 K with 8 K of hysteresis width. The asymmetric unit cells of the three polymorphs are almost identical and consist of one chiral complex molecule with the same configuration and conformation. The main differences between the structures of the three polymorphs are found in their crystal packing. The stabilization of the HS configuration for polymorph **B** is tentatively explained by the presence of two centers of steric strain in the crystal lattice resulting in the elongation of the Fe−N (aromatic) distance. The observed hysteresis in polymorph **C** has been attributed to the existence of an array of intermolecular contacts in the crystal lattice making the spin transition more cooperative than polymorph **A**. For the latter system based on the abpt ligand, there are two polymorphs, which crystallize in the monoclinic space group ($P2_1/n$). These complexes are very similar; however, there are two significant differences: (i) the average Fe−N bond distance is shorter for polymorph **A** by 0.03 Å, and (ii) the dihedral angle defined by the uncoordinated pyridyl group with the rest of the abpt ligand is 8.3° in polymorph

A, indicating that this molecule can be considered almost planar, whereas this angle is 34.5° for polymorph **B**. The quasi-planarity of polymorph **A** molecule stems from the formation of an intramolecular hydrogen bond between the nitrogen atom of the uncoordinated pyridyl group and the hydrogen atom of the 4-triazole-amine group. This singularity also dictates the distinct crystal packing. Thus, although polymorph **A** defines a one-dimensional array of molecules, a two-dimensional array is observed for polymorph **B**. Polymorph **A** undergoes SCO, and polymorph **B** (NCS^- derivative) remains HS up to ca. 0.4 GPa and successively undergoes a more complete spin conversion with higher characteristic temperatures, $T_{1/2}$. It is worthwhile mentioning that the SCO behavior of this polymorph **B** at 1.05 GPa is similar to that of polymorph **A** at 10^5 Pa. A singular example of polymorphism has been reported recently for the system $\{Fe[H_2B(pz)_2]_2phen\}$ ($[H_2B(pz)_2]$ = dihydrobis(pyrazolyl)-borate), where the photo-induced and thermal-induced HS states display different structures and consequently different polymorphs.[43] This system was found to be in the $C2/c$ monoclinic space group at 200 K where the compound is HS, but to undergo a loss of symmetry to a related primitive structure ($P\bar{1}$), with a unit cell volume approximately half that of the HS when the compound is cooled just below $T_c \approx 160$ K. This loss of lattice symmetry when the system goes from the HS configuration to the LS one leads to the loss of the C_2 molecular symmetry, a fact that probably favors the observation of thermal hysteresis. Interestingly, when the LS form is irradiated with red light at 30 K, it transforms into a second HS polymorph without the C_2 molecular axis ($P\bar{1}$).

In the present work, the synthetic method followed to obtain both polymorphs of the $[Fe(bt)_2(NCS)_2]$ system is slightly different from that reported by Ozarowsky et al.[27] These authors obtained polymorph **A** from slow evaporation of warm (78 °C) ethanol solutions; polymorph **B** crystallizes from evaporation of ethanol solutions at room temperature.[27] However, we have shown that crystals of both polymorphs, elongated black parallelepipeds and black octahedrons with cutoff corners, for **A** and **B**, respectively, can also be obtained by slow evaporation of ethanol solutions at room temperature.

The abrupt spin transition taking place within a few Kelvin accompanied with a 10 K hysteresis loop in **A** could occur concomitantly with a crystallographic phase transition like that observed for $\{[Fe(ptz)_6](BF_4)_2\}$[44] or in $\{Fe[H_2B(pz)_2]_2$-$phen\}$[43] among others.[1] However, it is also well-known that abrupt spin transitions are observed without a change in the crystallographic space group, as in $[Fe(phen)_2(NCS)_2]$.[3,32] The crystal structure determination performed at 150 K for **A** has demonstrated that no change in the space group takes place concomitantly with the change in the spin configuration. Moreover, multitemperature X-ray determinations in **A** have shown that the volume variation of the unit cell due to the thermal contraction (dilation), V_T, is negligible in the measured temperature range. Hence, the variation of the volume of the crystal and that attributed to the SCO process is the same, $\Delta V = \Delta V_{SCO} = 28$ Å^3 per formula unit and is accompanied by a hysteresis of 10 K. The fact that $\Delta V = \Delta V_{SCO}$ is an unexpected observation for a monomeric compound undergoing strongly cooperative spin transition because usually V_T decreases noticeably from room temperature because of the thermal contraction (dilation).[31,32,44] In contrast, ΔV_{SCO} falls into the upper limit range of values expected for iron(II) complexes (15−30 Å^3)[3,13,31,32] being 36% bigger than that observed for the classical system $[Fe(phen)_2(NCS)_2]$ polymorph II, where ΔV_{SCO} is 18 Å^3.[3,32] In the latter system, ΔV and V_T per complex molecule are 35.7 and 17.7 Å, respectively. Consequently, almost 50% of the volume change is due to the thermal contraction (dilation) and takes place progressively in a large interval of temperatures (300−130 K). In contrast, the change in the volume observed in **A** occurs just around T_c where the cell parameters a, b, and c experience a change similar in magnitude (0.3750(4), 0.3660(6), and 0.4030(8) Å, respectively) but different in sign, because b expands and a and c contract. This correlates quite well with distribution along the three directions of the strongest and the weakest intermolecular S···S contacts, respectively. The former contacts are found to be within the $a + b$ direction with a major component in b, and the latter contacts along the a and c directions. In $[Fe(phen)_2(NCS)_2]$ polymorph II, strong $\pi-\pi$ interactions are observed in the (a, b) plane and are mainly oriented in the b direction (ten C···C contacts ranging 3.40−3.52 Å), and only one contact is observed in the c direction (S···C = 3.36 Å). Thermal variation on a, b, and c parameters shows strong anisotropy according to the distribution of the intermolecular contacts. In fact, a contracts drastically around T_c (0.391(2) Å), whereas b slightly contracts from 300 K until T_c, after which it expands during the spin transition but ends in a total contraction at 130 K of 0.073(2) Å. The parameter c continuously contracts by 0.258 Å in the whole temperature range investigated (300−130 K).

Despite the fact that compound **A** and $[Fe(phen)_2(NCS)_2]$ polymorph II show similar spin crossover parameters (T_c, ΔH, ΔS, ΔV) and strong intermolecular interactions and remain in the same space group whatever the temperature, their response to applied hydrostatic pressures is dramatically different. In $[Fe(phen)_2(NCS)_2]$ polymorph II, as pressure is increased, the transition curve shifts to higher temperatures with an average dependency of 220 K/GPa. With the application of pressure, the narrow hysteresis loop disappears and the transition curves become gradual. At pressures around 0.6 GPa, the sample is mostly in the LS state at room temperature.[32b] Meanwhile, the response of polymorph **A** under applied pressure is quite unusual and can only be understood in terms of the occurrence of a crystallographic phase transition or a change in the bulk modulus of the material, as has been proposed for $[Fe(phy)_2](ClO_4)_2$,[45] $[Fe(PM\text{-}Bia)_2(NCS)_2]$,[46] and $\{Fe(pmd)(H_2O)[Ag(CN)_2]_2\}\cdot H_2O$.[5] For these systems, an increase in hysteresis width, crystallographic phase transitions, and nonlinear hysteretic behavior of $T_c(P)$ versus pressure, respectively, have been reported. In order to gather deeper insight of such unexpected pressure effects, crystal structure determination under applied pressure and, of course, at variable temperatures would be necessary. However, the experimental difficulties involving pressure and

temperature-dependent crystal structure determinations are well-known. Nowadays, high-pressure structural properties of only three SCO Fe(II) systems[40,47] and one SCO Mn(III) complex have been reported.[48]

It is worthwhile mentioning the discrepancy found between the pressure experiments reported in ref 28 and in the present work with regard to polymorph **A**. In ref 28, the authors found a linear shift of $T_c(P)$ vs P in the range 10^5 Pa to 0.2 GPa.[28] In contrast, in the present work, we have evidenced a nonlinear dependence of $T_c(P)$ vs P under strict hydrostatic pressure conditions. This discrepancy could be ascribed to the possible nonhydrostaticity of the pressure cell construction used in ref 28. Indeed, similar related discrepancies have been previously reported.[33,34,45]

As far as polymorph **B** is concerned, the crystallographic data indicate that this polymorph crystallizes in a more symmetrical $C2/c$ space group instead of the $P\bar{1}$ triclinic space group indicated in the previous work.[27] Consequently, the crystal packing described in the cited work for polymorph **B** is quite different from that depicted here.

Finally, a surprising result from the present investigation is the paramagnetic behavior of **B** even at relatively high pressures such as 1.06 GPa. This result strongly contrasts with the high-pressure studies performed on the above-mentioned polymorph **B** of the [Fe(abpt)$_2$(NCX)$_2$] system. At 1.05 GPa, this polymorph undergoes a spin transition similar to that observed for the corresponding polymorph **A** at 1 bar. For these polymorphs, the differences in average bond length and trigonal distortion parameter are 0.03 Å and 4.7°, respectively (ϕ(**A**) = 8.5°, ϕ(**B**) = 13.2°). The higher the value of ϕ, the more stable the HS state results.[1,2a,3,47] Taking into account that the difference in the averages of the bond length and the trigonal distortion parameter between **A** and **B** are 0.009 Å and 5.1°, it should be expected that pressures as high as 1.0 GPa should induce the change in the spin configuration. Therefore, the hypothesis of a pressure-induced crystallographic phase transition becomes plausible in order to explain the response of **B**. Seemingly, application of pressure induces a new crystallographic phase in which the HS configuration is favored.

In summary, the structural analysis of polymorph **A** points out that no change in the space group accompanies the abrupt spin transition and that the change in the volume of the crystal is mainly due to the spin crossover process. Pressure experiments on **A** demonstrate a nonlinear behavior of $T_c(P)$ vs P, which could be understood in terms of crystallographic phase transitions under applied pressures. For **B**, application of hydrostatic pressures seems to stabilize the HS configuration.

Acknowledgment. Financial support is acknowledged from the Spanish Ministerio de Educacion y Ciencia (MEC) (CTQ 2004-03456/BQU) and from the Generalitat Valenciana for the research grant ACOMP06/048. A.G. thanks the Universitat Politécnica de València for a predoctoral fellowship. A.B.G. thanks the Spanish MEC for a research contract (Programa Ramón y Cajal). We thank Dr. V. Ksenofontov for helpful discussions.

Supporting Information Available: CIF data for polymorphs **A** and **B**. DRX pattern for polymorph **A** and **B** at 293 K. This material is available free of charge via the Internet at http://pubs.acs.org.

IC060729U